JOURNAL OF MATERIALS SCIENCE, 29 (1994) 3542–3552

Ion-bombardment modification of surface morphology of solids

Part 2 *Changes in surface shape*

ZBIGNIEW W. KOWALSKI
Technical University of Wrocław, I-25, 50-370 Wrocław, Poland

Ion bombardment modification of surface geometrical structure, i.e. surface roughness alteration (Part 1) and changes in surface shape (this paper) are considered. Two surface shape alteration methods, masked and maskless pattern etching, are described. They have been applied to modify various kinds of targets, including metals (99.9% aluminium and 99.9% titanium), metal alloys (stainless steel of 1H18N9T and SS 316 LC), alumina ceramic (96% Al_2O_3) and Teflon. The results of experiments, where narrow beam glow discharge (GD) and broad beam Kaufman type guns have been used as ion sources, are presented. Approximation of a real surface shape profile by a so-called "mean line", which is very helpful in the case of ion patterned but extremely rough surfaces, is also discussed. Finally, the practical aspects of ion bombardment modification of surface shape phenomenon, i.e. its application to sputtering yield and sputtering velocity measurements, are shown.

1. Introduction

It is well known that ion sputtering of solid surfaces causes modification of geometrical features, such as roughness and shape; these are the main aspects of a much more complex phenomenon termed ion bombardment modification of surface morphology [1]. The influence of ion irradiation on surface roughness has been discussed in Part 1 of this paper [2]. Here ion bombardment induced changes of surface shape are presented.

It should be remembered that each surface contour consists of both surface roughness and surface shape profiles. The criterion of this classification is a quantity of coefficient f, where

$$f = \frac{D}{H} \tag{1}$$

where D is a mean distance between two following surface protuberances (surface contour maxima) and H is the height of the largest (extreme) protuberance (see Fig. 2 in Ref. 1). The studied contour is considered as a surface shape profile for $f \geqslant 1000$.

Ion beam technology provides various methods of surface morphology modification. The most often utilized is natural sputtering, NSput, where the sputtered sample (target) is placed directly in the region of ion beam. The beam is characterized by constant spatial distribution of ion current density, j, and by different inclinations to the surface, θ: from $\theta = 0$ rad ($NSput_0$) to 0 rad $< \theta \leqslant \pi/2$ rad ($NSput_\theta$). The natural sputtering method can be applied to modify the surface roughness and reveal surface structure [1].

Another method is seed texturing, STex, i.e. ion sputtering with a sputter resistant material (seed material) supplying the target surface during ion irradiation. Normal ion beam incidence ($\theta = 0$ rad), constant spatial distribution of ion beam current density and seed material in the form of a plate located in the proximity of the target are the main features of this method. STex is commonly used to generate cone- or pyramid-like textures on ion bombarded target surfaces.

A further method termed pattern etching, PEtch, enables alteration of surface shape, and is described in detail in this paper.

2. Surface shape alteration

2.1. Characteristics of ion beam pattern etching

Among different pattern etching techniques, such as plasma etching (PE), reactive ion etching (RIE) or ion beam etching (IBE), which are known to be good methods for the fabrication of devices with micrometre or even submicrometre dimensions, IBE (considered here as ion beam pattern etching, IBPE, technique) is remarkably versatile. It has the following advantages over PE and RIE [3]:

1. The energy and current density of ions in IBPE can be varied independently;

2. The target surface can be irradiated at any desired angle θ. This is very important because of the strong dependence of sputtering yield, Y, of most materials on angle θ. A typical curve of $Y(\theta)$ shows a maximum $Y(\theta_m)$ at 0.85 rad $\lesssim \theta_m < \pi/2$ rad and declines to zero at $\theta_n = \pi/2$ rad (Fig. 1).

3. The gas pressure in the target chamber can be kept low enough to reduce pressure induced secondary effects.

0022–2461

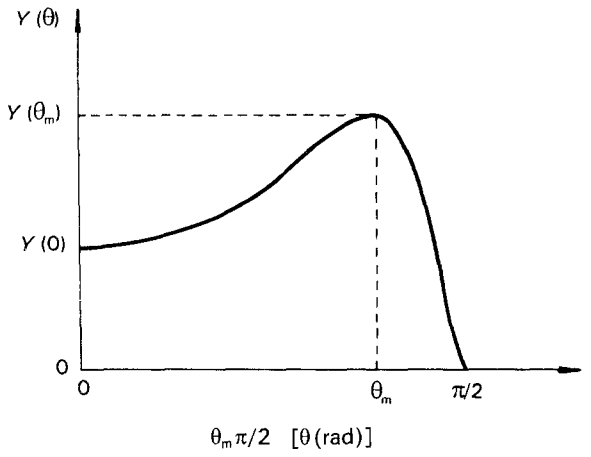

Figure 1 Typical shape of sputtering yield curve $Y(\theta)$.

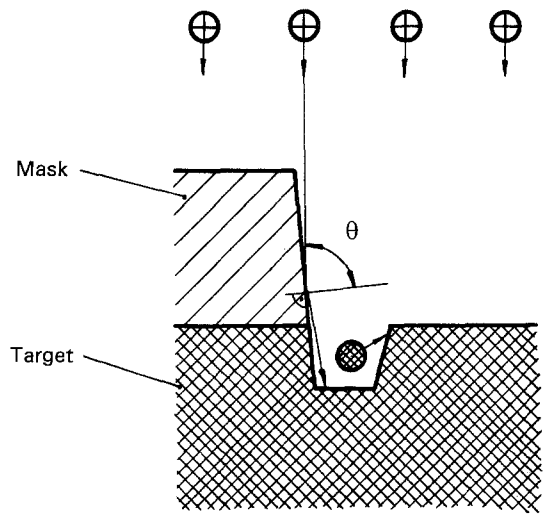

Figure 3 The effect of enhanced erosion (or trenching) near the base of vertical wall of mask caused by ion reflection from the wall. Angle of ion incidence $\theta \leqslant \pi/2$ rad. ⊕ = ion, ⊛ = target atom.

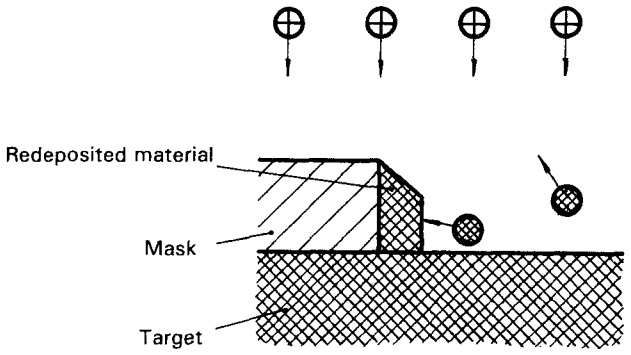

Figure 2 The effect of redeposition of sputtered material onto a vertical wall of a metallic mask (or resist) during ion beam etching at normal incidence. After removal of the mask, the side metallic walls of redeposited material may remain and interconnect isolated regions producing short circuits or related effects. ⊕ = ion, ⊛ = target atom.

4. It is possible to etch insulating materials, provided that the positive charge which accumulates on ion irradiated surfaces of non-conductive target materials is neutralized during ion etching by electron bombardment.

However, there are some disadvantages of IBPE which are, or may be, important for device applications [4]:

1. redeposition of sputtered material (Fig. 2);
2. ion reflection (Fig. 3);
3. bombardment induced damage;
4. preferential sputtering;
5. relatively small etch selectivity.

Each practical application requires the consideration of both the advantages and limitations of the IBPE technique.

IBPE is practically realized by means of a showered ion beam (SIB) or a focused ion beam (FIB). Among various experimental configurations of IBPE two main methods can be distinguished. The first involves the use of various masks, the patterns of which ought to be transferred with high fidelity onto the ion etched target surface [5, 6]. The second does not use masks but modifies surface shape by: (a) a highly collimated beam [7–9] which engraves patterns on a target material; (b) a condensed beam which passes through the image forming lens and creates a demagnified image of given pattern on the target material surface; (c) a beam of spatially changing ion current density which induces (projects) the shape of target surface resembling the above ion current density distribution shape [10, 11].

2.2. Masked IBPE

Masked ion beam pattern etching, schematically represented in Fig. 4, is considered here as the process whereby various types of masks, having certain patterns, are transferred onto a target surface and utilized with intimate contact with the surface during ion etching, i.e. 1 : 1 shadow printing with ions. For submicron resolution, submicron masks are required which are subjected to the same power density as the target [6].

The masked IBPE method can be utilized in various ion beam processes, such as [12]: (a) ion beam mask etching (physical sputtering through masks, pattern generation by reactive ion beam etching); (b) ion beam slope cutting; (c) ion beam microfiguring (sputtering through movable screens, ion beam microlathing).

One of the simplest changes of surface shape by means of masked IBPE is formation of a step (Fig 5). The border between initial (i.e. masked during the etching process) and ion irradiated surfaces is a good source of information about ion beam pattern etching itself (etching rate, sputtering yield, secondary effects, etc.) as well as about results of the process (modification of surface topography and roughness, creation and/or revealing of macrodefects, etc.). Generally, two main examination tools are used to study geometrical properties of the etched surface, for instance a step with an adjacent surface area: (a) profilograph (conventional with mechanical stylus, e.g. Planer Industrial's SF 220 Surface Profiler, or non-contact and non-destructive, e.g. Rodenstock's Optical Surface Measuring System RM 600); (b) microscope (optical,

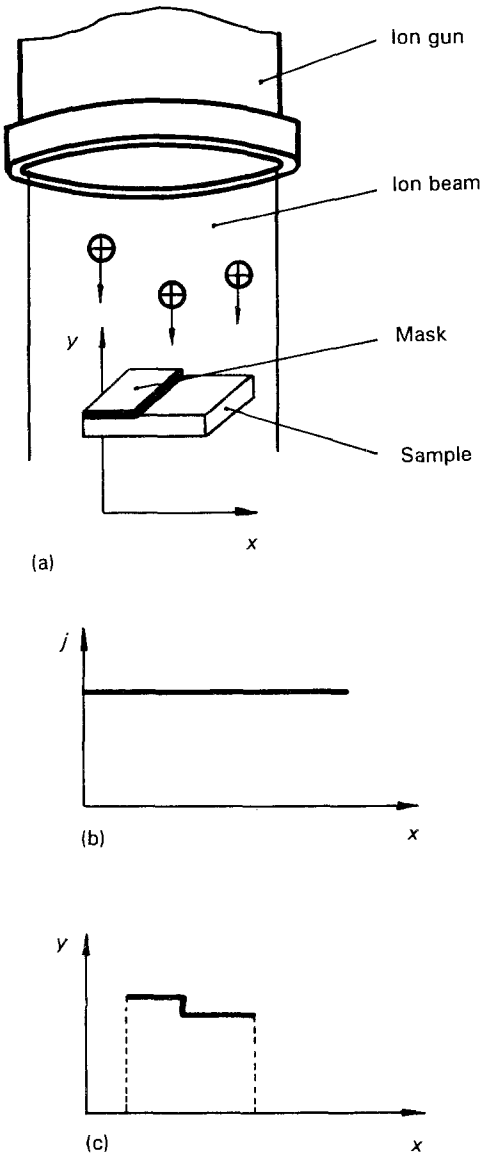

Figure 4 Schematic representation of the masked ion beam pattern etching (IBPE) method of modification of a sample surface shape. (a) The basic variant of IBPE where different types of masks are used (here the simplest one in the form of a plate is shown as an example); (b) the dependence of ion beam current density, j, on distance, x (j = const); (c) a real surface profile (in x-direction) of the sample after ion etching with the simplest mask.

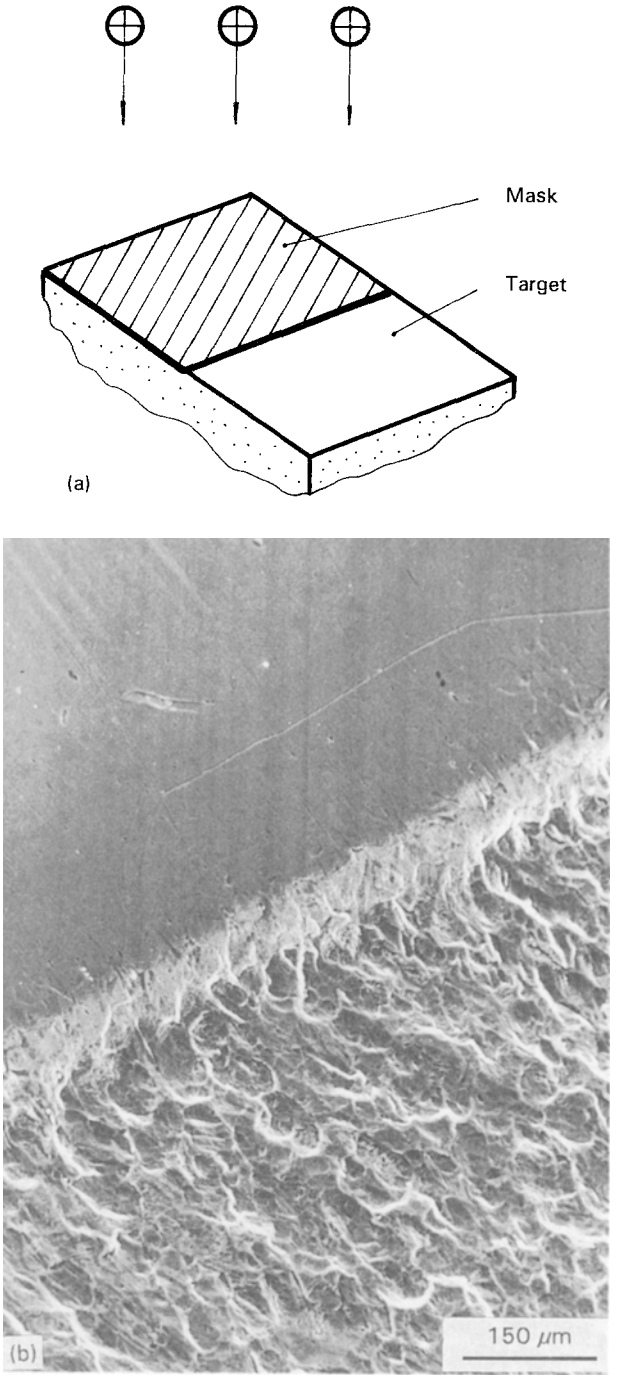

Figure 5 Modification of surface shape of a sample by means of ion beam etching through a simple mechanical mask. (a) A method of step formation; (b) photograph (SEM, JEOL, JSM-35) of the step on a surgical chrome–nickel stainless steel surface caused by a broad ion beam sputtering process (0.8 mA cm^{-2}, 1 kV, 600 min) [5].

scanning electron and scanning force (used as a profilometer), e.g. SFM for operation in air of Park Scientific Instruments).

An example of a more complicated change of surface shape is seen in Fig. 6. This scanning electron microscope image shows the pitted surface of a selected area of a wide plate of type 63018 (OSTEO AG, Selzach Products, 1976) used in orthopaedic surgical operations to join broken bones. To modify the surface of this orthopaedic implant, screen mesh with micrometre apertures has been used as a mask. To ensure the precise projection of the aperture onto the sputtered surface it is important to hold the screen in intimate contact with the sample and to make the mesh of a sputter resistant material. The sputtering yield of the screen mesh relative to the target material determines the maximum depth to which the pits (pores) can be etched prior to complete sputter loss of the mesh. It means that the higher the sputtering yield of the target (sample) material the deeper the pores can be etched.

The two examples given above are able to adequately characterize the masked IBPE method. However, ion beam pattern etching together with lithography techniques allows countless numbers of possible surface shapes to be obtained with extremely small dimensions. Masked ion beam lithography (MIBL) is such a submicron pattern replication technique (first reported in 1974) which has a high

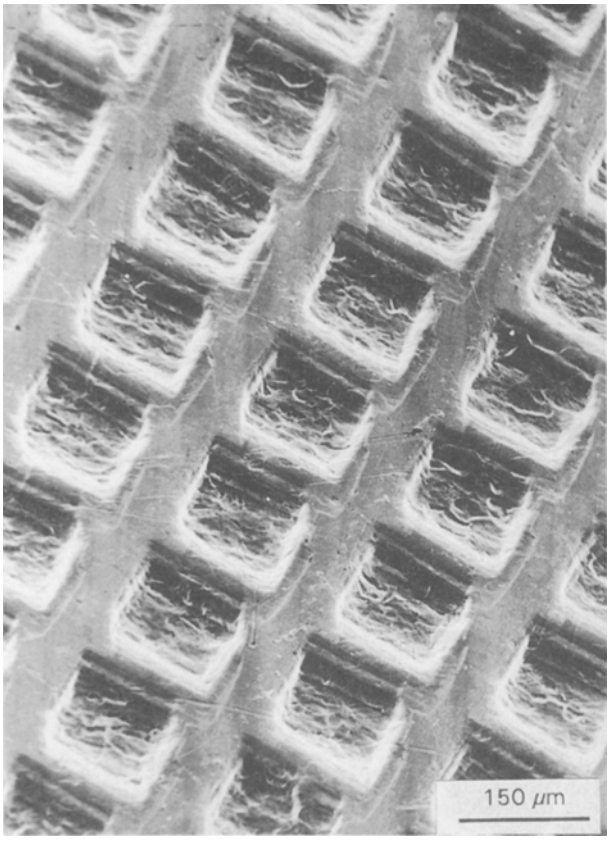

Figure 6 Pitted surface of chrome–nickel stainless steel used for orthopaedic implants (it corresponds to the American standard AISI 316LC) resulting from 210 min of ion beam pattern etching through the stainless steel screen mask from a Kaufman-type source (1000 V, 2 mA cm^{-2}) [5].

throughput capability, up to 60 100 mm wafers h^{-1} with 0.1 μm alignment and 0.1 μm resolution [13]. The collimated beam of 50–250 keV floods a large area (1–2 cm^2) lithography mask which is in close proximity to a resist coated wafer. An all-silicon mask (where the absorbing and transmitting patterns are regions of thicker and thinner silicon, respectively, in one monolithic structure) and a stencil mask (made of etched patterns in metal foils) were technologies developed for the fabrication of masks for MIBL. Unlike the all-silicon masks, the stencil and open masks have excellent contrast, i.e. ions are not scattered while passing through the open holes.

An important problem is one of ultimate resolution of ion beam lithography (also MIBL). Among the factors which determine the resolution, primary ion scattering, recoil atom scattering and the finite range of ion beam induced secondary electrons seem to be of great importance [6].

During interaction with a solid, ions scatter and lose energy through nuclear and electronic scattering processes. The total energy loss $(dE/dx)_T$ is given by:

$$\left(\frac{dE}{dx}\right)_T = \left(\frac{dE}{dx}\right)_N + \left(\frac{dE}{dx}\right)_E \quad (2)$$

where $(dE/dx)_N$ and $(dE/dx)_E$ are the nuclear and electronic stopping powers, respectively.

It is well known from the collision theory that both terms (i.e. nuclear and electronic) in Equation 2 depend on the atomic mass of the primary ion, its energy and the atomic mass of the target atom. For heavy ions bombarding light or heavy targets, the dominant mechanism of energy loss is nuclear, with significant beam spreading. For low energy (few keV), light ions incident on light materials (e.g. resists) the dominant mechanism is electronic with minimal sideways scattering. For lithography the second mechanism is much more useful because it enables lateral scattering effects to be minimized.

The other phenomenon which affects the lateral exposure is the recoil of the target atoms, which occurs more readily with incident heavy ions than with light ones. Unfortunately, heavy ions interact with resists via nuclear interactions, producing a large number of recoils. Light ions are much more interesting because they interact with resist materials via an electronic mechanism (recoils are not generated).

A further contribution for lateral exposure is due to secondary electrons emitted from a target material under ion bombardment by two processes – potential (velocity of an impinging primary ion below 10^5 m s^{-1}) and kinetic (velocity higher than 10^5 m s^{-1}) emission mechanisms. At energies above 10 keV the important mechanism for secondary electron production is considered to be kinetic emission [6].

2.3. Maskless IBPE

The term 'maskless IBPE' is used here to describe ion beam etching processes where masks in intimate contact with patterned sample surface containing and storing the complex design patterns that should be printed with ions on target surface are not used.

Among various possible methods of maskless IBPE the use of ion beams of spatially changing ion current densities is the simplest. The idea is to induce a surface shape profile which resembles a certain ion current density distribution (Fig. 7). This method has been successfully used for more than three decades in sample preparation for transmission electron microscopy (TEM). The concept was developed in 1961 by Paulus and Reverchon [14]. Their apparatus consisted of vacuum enclosure containing two hollow anode d.c. glow discharge (GD) guns. The specimen to be prepared for TEM was ion beam etched until a small perforation was electron transparent (the area of interest for TEM studies). During the last 30 years several ion beam machines for specimen preparation with various ion sources (e.g. GD with hollow anode, saddle field or Steigerwald type guns) and equipment have been manufactured and sold as commercial units.

In this method of IBPE the projection of ion current density distribution on the ion beam bombarded target surface is far from perfect, but is adequate in practice. Fig. 8 shows the profile of a funnel-shaped pit etched on a Corning 7059 glass surface by an argon ion beam from a d.c. GD ion gun with a hollow anode [10]. Unfortunately, the accuracy of the projection (examined, for example, by a simple method shown in Fig. 9 for a perpendicular argon ion beam bombardment of Corning 7059 glass surface) is insufficient for

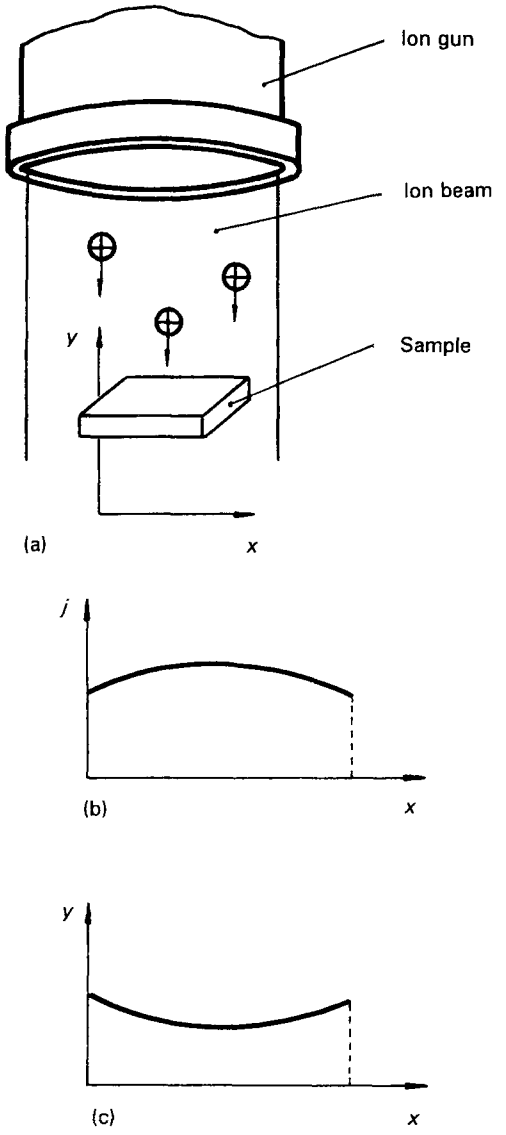

Figure 7 Schematic representation of maskless ion beam pattern etching method of modification of a sample surface shape. (a) The basic variant of the method where an ion beam of spatially changing ion current density is used to induce a surface shape resembling that ion current density distribution; (b) the dependence of ion beam current density, j, on distance, x; (c) a real surface profile (in x-direction) of the sample after a maskless IBPE process. ⊕ = ion.

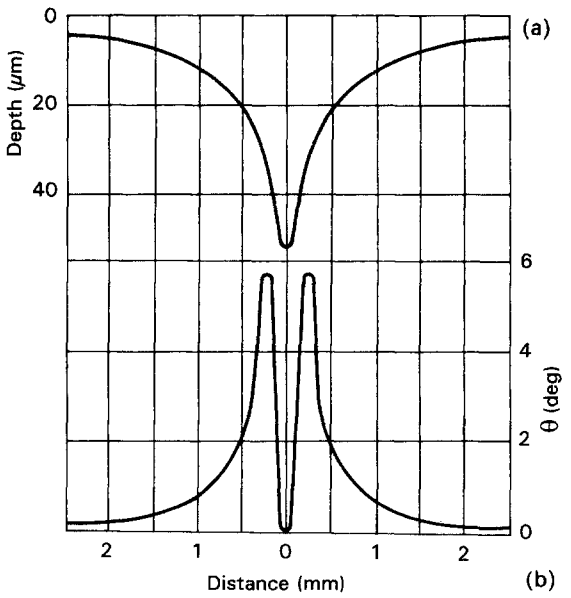

Figure 8 The funnel due to perpendicular beam etching for 1 h at a distance of $x = 10$ mm. (a) Funnel profile; (b) true inclination of the funnel slope (for more information see Ref. 10).

the production of modern and unique structures with nanometre dimensions, or in other maskless fabrication techniques.

The development of focused ion beam (FIB) systems based on liquid–metal and gas field ion sources [9, 15], generating beams with a spot size down to several nanometres [16], removed this difficulty and opened up a new area of possible applications of ion beam technology, such as ion microprobe and secondary ion mass spectrometry, ion microscopy, lithography, ion implantation and doping, deposition and mask repair, as well as (especially interesting here) micromachining, microfabrication and ion beam etching. FIB systems can be used to write a pattern on a substrate (by changing doses locally) with nanometer precision. For this the stage motion and the beam deflection need to be integrated, which can be done by computer. Experiments have demonstrated the potential of FIB technology to be used in the formation of uniform holes and inclined facets [12], program-controlled production of three-dimensional optical surfaces (Fig. 6.30 in Ref. 12), in mask making or in direct writing for submicron feature devices on a wafer (e.g. the 0.1 μm resist patterns were successfully fabricated on both PMMA and CMS resists on Si and SiO_2 substrates [17]; patterned substrates suitable for epitaxial growth were produced by direct-write lithography process for InP wafers in which a finely focused Ga^+ ion beam was used to form the pattern which was then transferred into the substrate by dry etching [18]). Other interesting applications of FIB technology can be found in the comprehensive literature [9, 15, 19].

A typical FIB system consists of three main parts [13]:

1. the ion source (liquid–metal ion (LMI) or gas field ion source [GFIS]);
2. the ion optics column (objective lens, aperture, first stigmation and alignment deflector, beam blanker, second stigmation and alignment deflector, projector lens, quadrupole deflector, octupole deflector);
3. the sample stage (driven on special bearings by computer controlled electric motors and positioned by means of a laser interferometer with 0.01 μm accuracy).

The system is characterized by [13, 16]: acceleration voltage 3–200 kV, current density up to 10 $A\,cm^{-2}$, probe current 10–300 pA, and ion species: Ga^+, Au^+, Si^+, Be^+, B^+, As^+, P^+, etc.

Advantages such as pattern creation and modification performed by computer, high sensitivity, very low proximity effects and high resolution (11–14 nm wide patterns can be formed [16]) make FIB lithography very attractive. The major disadvantage of the technique is low throughput (its writing speed is limited by the kinetics of heavy particles).

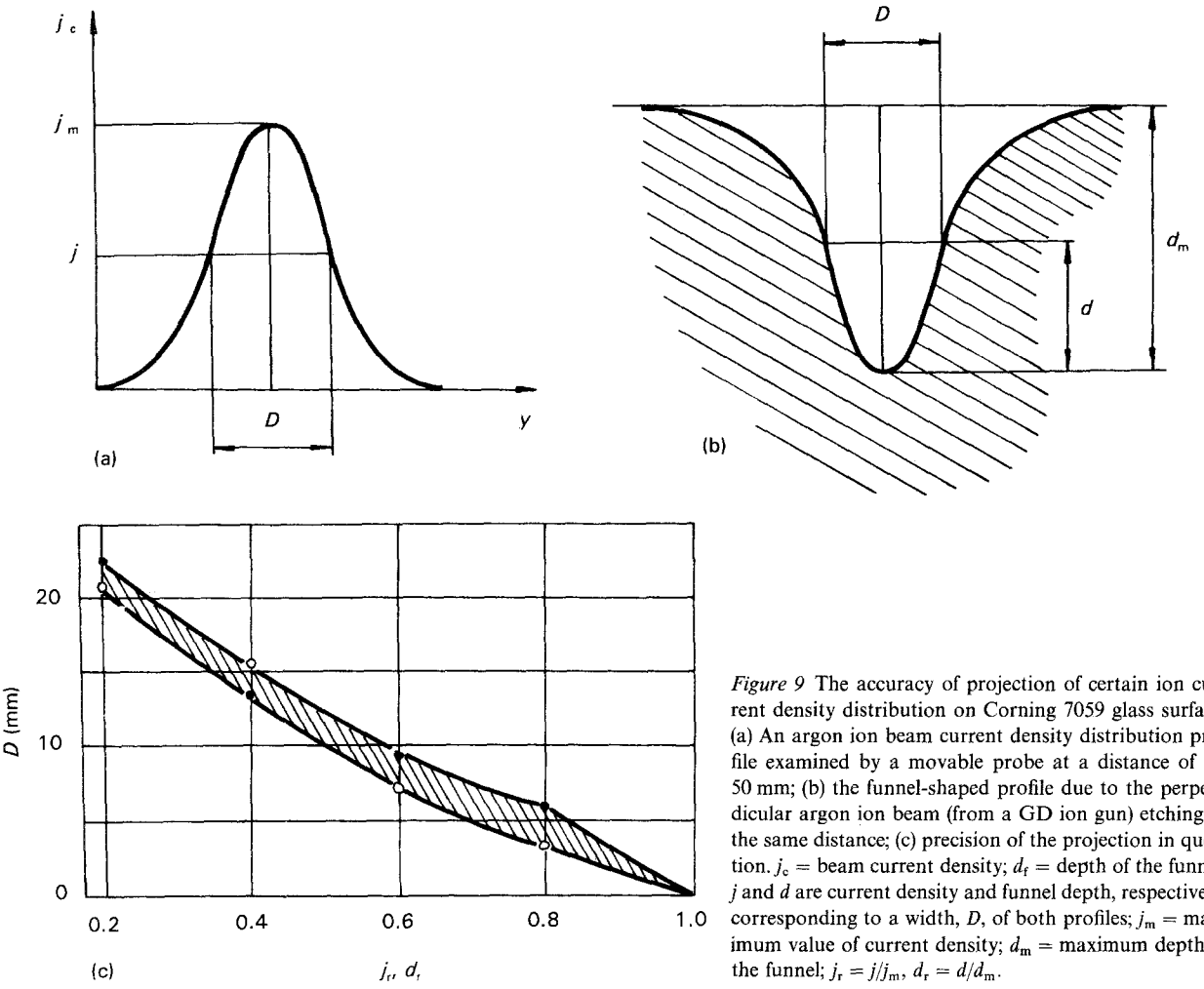

Figure 9 The accuracy of projection of certain ion current density distribution on Corning 7059 glass surface. (a) An argon ion beam current density distribution profile examined by a movable probe at a distance of ca. 50 mm; (b) the funnel-shaped profile due to the perpendicular argon ion beam (from a GD ion gun) etching at the same distance; (c) precision of the projection in question. j_c = beam current density; d_f = depth of the funnel; j and d are current density and funnel depth, respectively, corresponding to a width, D, of both profiles; j_m = maximum value of current density; d_m = maximum depth of the funnel; $j_r = j/j_m$, $d_r = d/d_m$.

Another modern maskless IBPE technique called ion projection lithography (IPL), or image-projection ion beam lithography [20], can be used to perform:

1. direct structuring without any resist with high throughput (the ion exposed area of material is physico-chemically modified due to the induced radiation damage and as a result it is etched faster than the initial one);
2. submicron patterning of resist layers.

A typical IPL system consists of: an ion source, a stencil mask (patterns of which should be demagnified by 10:1, for example), an immersion lens, an octupole, a projection lens system, an X–Y stage, and, of course, power supplies and a vacuum system. Demagnifying projection avoids the problems of submicron mask production and maintenance, as well as causing the ion energy and current density being higher at the sample surface (wafer) than at the mask. The main limitation of IPL is the optics [6].

IPL is the technique [13] where a condensed ion beam, accelerated by an electrostatic lens, passes through the image forming lens and creates a demagnified image of mask patterns on the wafer. Typical beam densities are 0.5–3 mA cm^{-2} on the chip, exposure time ca. 10 min, alignment accuracy $\pm$ 0.05 μm and ion species as follows: H^+, He^+, N^+, Ne^+, Ar^+, etc.

It can be concluded that both FIBL and IPL are very promising maskless ion beam pattern etching techniques which may be applied to structure patterns of nanometre resolution (FIBL) and with an attractive throughput (IPL).

3. A mean line in surface shape studies

It can be assumed that both surface roughness and surface shape profiles are the major constituents of every surface contour of target material. There is no problem in identifying (by means of profilograph or microscope) the surface shape profile of smooth targets; however, difficulties arise with an increased roughness of surface, particularly in the case of extremely rough surfaces with patterns of micrometre or submicrometre dimensions. Such difficulties are encountered in microelectronics, where fine geometry devices are fabricated using masked or maskless IBPE techniques, and in implantology, where fine geometry devices can be applied as, for example, artificial teeth or bones. It is difficult to find the surface shape profile in such cases, and then to distinguish the surface shape from the surface roughness profiles. It seems that the determination of the so-called "mean line" (Fig. 10) would be a good solution to the problem [21]. This line could represent (approximately!) a real surface shape profile.

By definition the mean line is a line which divides a surface contour in such a way that in the range of a conventionally determined segment, L, the sum of

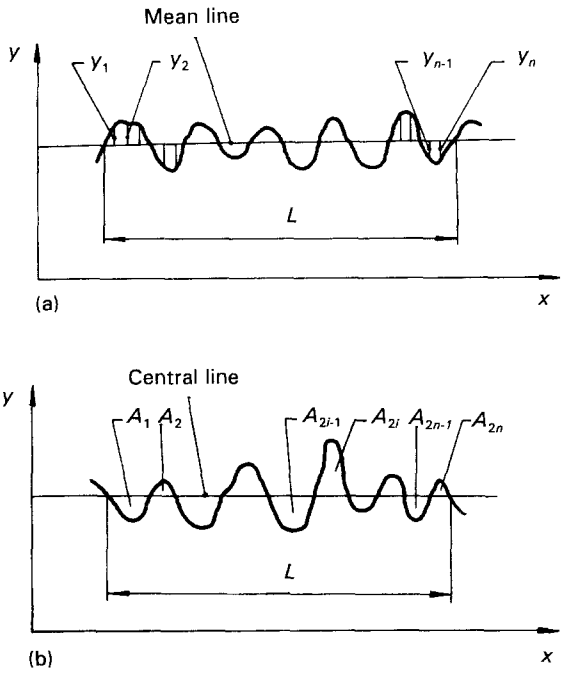

Figure 10 Schematic representation of (a) a mean line and (b) a central line, considered to be good approximations of a real surface shape profile.

the second power deviations, y_i ($i = 1, 2, 3, \ldots, n$), of the contour from this line is a minimum (Fig. 10a), i.e.

$$\sum_{i=1}^{n} |(y_1)^2 + (y_2)^2 + \cdots + (y_i)^2 + \cdots + (y_n)^2| = \min \quad (3)$$

In a graphical approximate determination of the mean line it is convenient to find a so-called "central line" (Fig. 10b), i.e. a line dividing a surface contour in such a way that, in the range of a conventionally determined segment, L, the sum of areas, A, which are contained between this line and the contour, is the same on both sides of the line, i.e.

$$\sum_{i=1}^{n} A_{2n-1} = \sum_{i=1}^{n} A_{2n} \quad (4)$$

Fig. 11 shows an example of a possible use of a mean line to evaluate the correctness of a surface shape obtained after an IBPE process. Here a groove of constant cross-section is considered. Fig. 11a presents the shape of a real surface to be developed by an IBPE process; two results of ion patterning, firstly in accordance with the project and secondly considerably different, are shown in Fig. 11b and c, respectively. In both cases, and especially in the latter, a mean line can be very helpful in obtaining an approximate profile of a real surface shape of an ion etched groove. It is not difficult to find experimental examples of IBPE surfaces which illustrate and confirm the theoretical cases presented in Fig. 11. To obtain surgical implants with specially modified surface geometrical structures IBPE processes have been applied [22]. By using screen mesh masks, surfaces with a uniform pattern structure should be fabricated. Contrary to these optimistic expectations, the surface topography observed at the bottom of individual pits is not uniform and differs from pit to pit. This unique topography depends on many factors. Among them material properties, the etch rate of the screen mesh relative to the target material and sputtering conditions are probably very important. Fig. 12 shows one of the pits selected from an IBPE surface (Fig. 12a) of a given material, for example, the surface of an orthopaedic implant (Fig. 12b) made of chrome–nickel stainless steel of type 316LC (American standard AISI) or an SEM image of a pit resulting from etching of a Teflon surface (Fig. 12c). In spite of the 'almost smooth' surface of the untreated area of a sample (beneath the mask), the surface of the pit bottom of stainless steel in Fig. 12b is rough and it is therefore difficult to determine the real surface profile. The situation is much more complicated with Teflon (Fig. 12c) etched by the same method. In addition to the rough initial (unsputtered) surface, the bottom of the pit is extremely rough

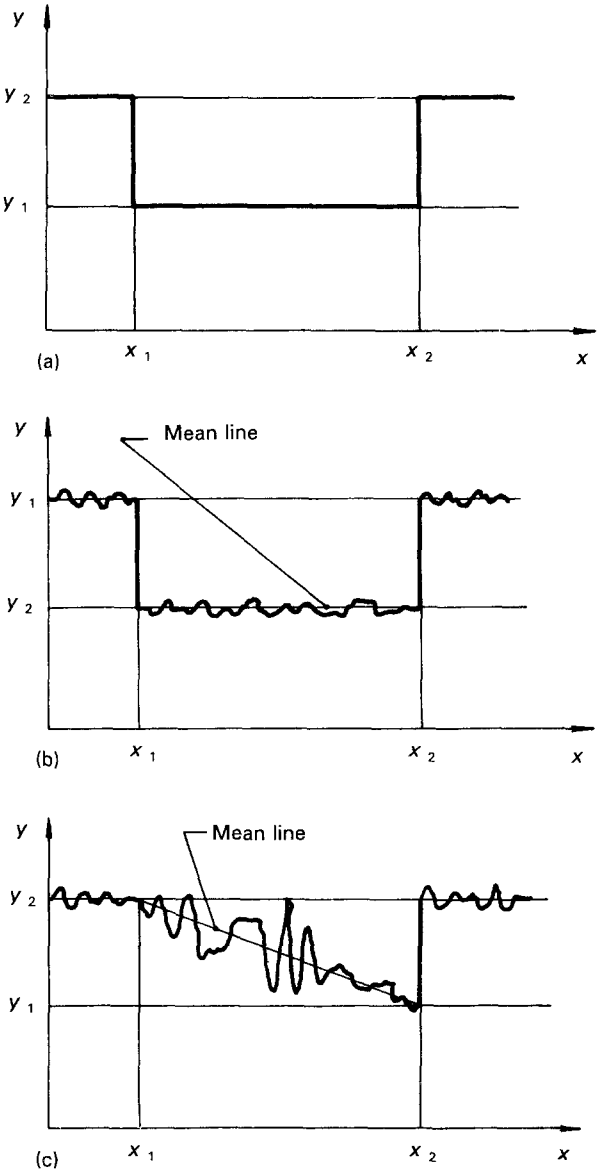

Figure 11 An example of possible use of a mean line to evaluate the correctness of a surface shape obtained as a result of ion beam pattern etching. (a) The shape of a real surface which is projected, e.g. a groove of constant cross-section; (b) the surface shape obtained in accordance with the project, disturbed by topographical elements; (c) a surface shape obtained due to an IBPE process which is considerably different to the projected one.

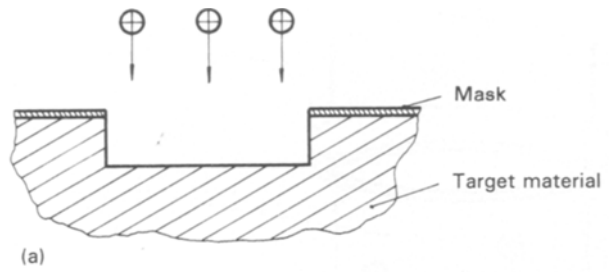

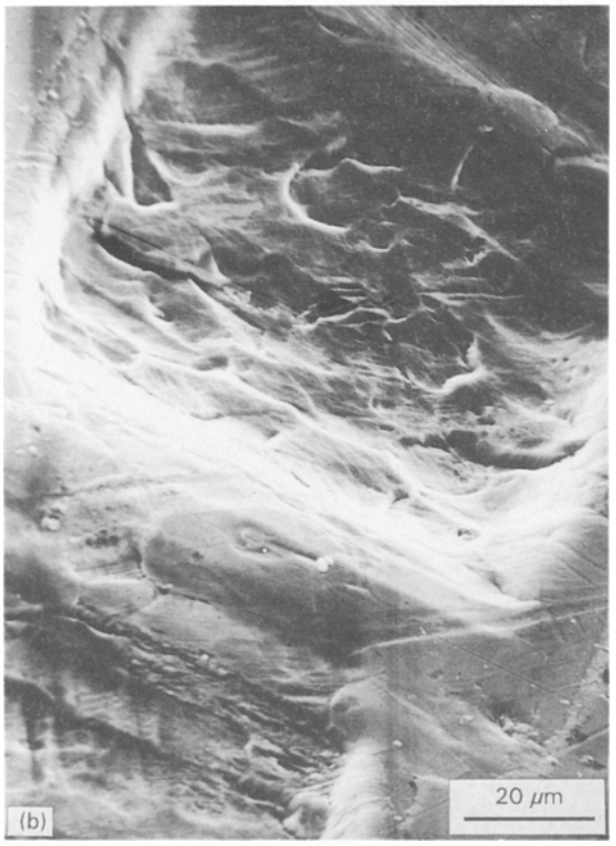

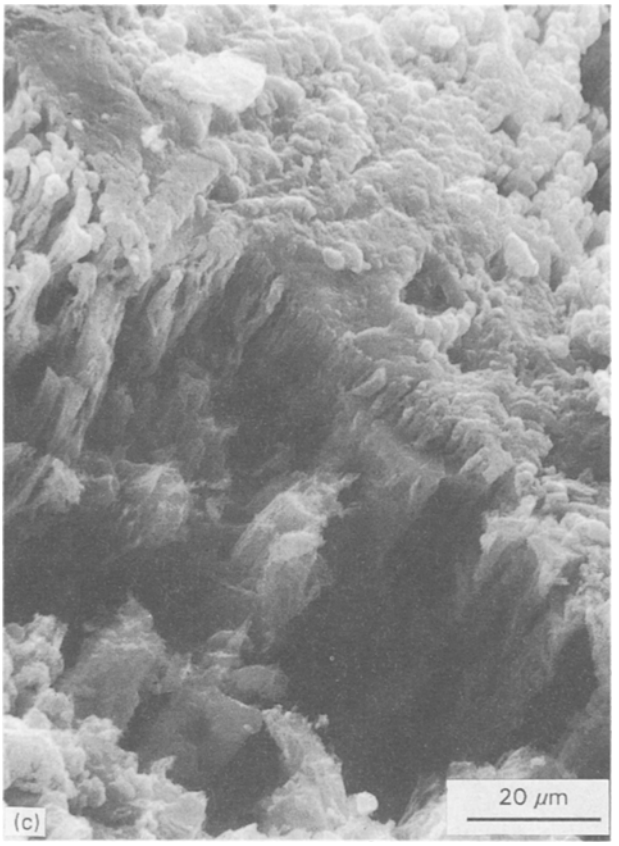

Figure 12 Modification of the surface shape of various materials [1] – experimental verification of the two cases of pattern etched surfaces from Fig. 11b and c. (a) Schematic representation of the ion beam patterning technique used in the experiment; (b) a depression etched (2 mA cm^{-2}, 1 kV, 210 min) in chrome–nickel surgical stainless steel; (c) a distinct misshapen depression etched in a Teflon surface (0.5 mA cm^{-2}, 1 kV, 90 min). ⊕ = ion.

and the dimensions of the topographical features formed on the bottom during the IBPE process are similar to the pit dimensions. It is difficult to find the surface shape profile in such a case, and then to distinguish it from the surface roughness profile, without the help of the mean line.

Many other topographical features can be observed at the bottoms of individual pits, depending on ion beam patterned material and ion bombardment conditions used in the experiment. Fig. 13 presents, as an example, different aspects of surface topography modification observed on patterned parts (bottoms of particular depressions) of titanium sample, i.e. simple elements of cone texture probably generated by means of seed texturing mechanism (Fig. 13a) and elements of revealed surface macrostructure (grains, Fig. 13b) which also make it difficult to find the real surface shape profile induced by the IBPE process.

4. Sputtering yield and velocity measurements

Changes in the surface shape profile induced by IBPE can be utilized to provide sputtering yield and velocity measurements. To investigate these changes a so-called "3S" method, described elsewhere [23], has been proposed. It differs from the conventional manner in that only one specially shaped sample (Fig. 14) and only one ion irradiation process can be used to determine the changes mentioned above. The term "3S" comes from the specially shaped samples used in the method. It seems that "3S" is a good, simple and relatively inexpensive, but approximate(!), technique which is particularly useful in the first stage of study of a new material. Fig. 15 shows the erosion of unit area, A, of the target surface after unit time, dt, of ion beam bombardment through the etching (sputtering) resistant mask. Using the definition of sputtering yield

$$Y = \frac{N_a}{N_i} \tag{5}$$

with

$$N_a = nA\,dR \tag{6}$$

and

$$N_i = \phi\,dt \tag{7}$$

where N_a and N_i are average numbers of ejected atoms and incoming ions, respectively; n is the number of atoms per unit volume of target material; dR is the breadth of step formed on the border between the

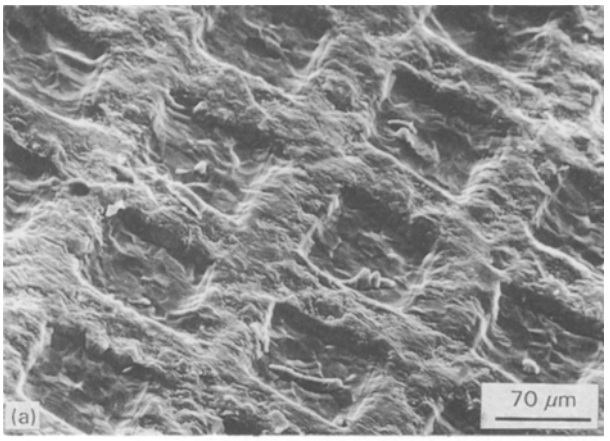

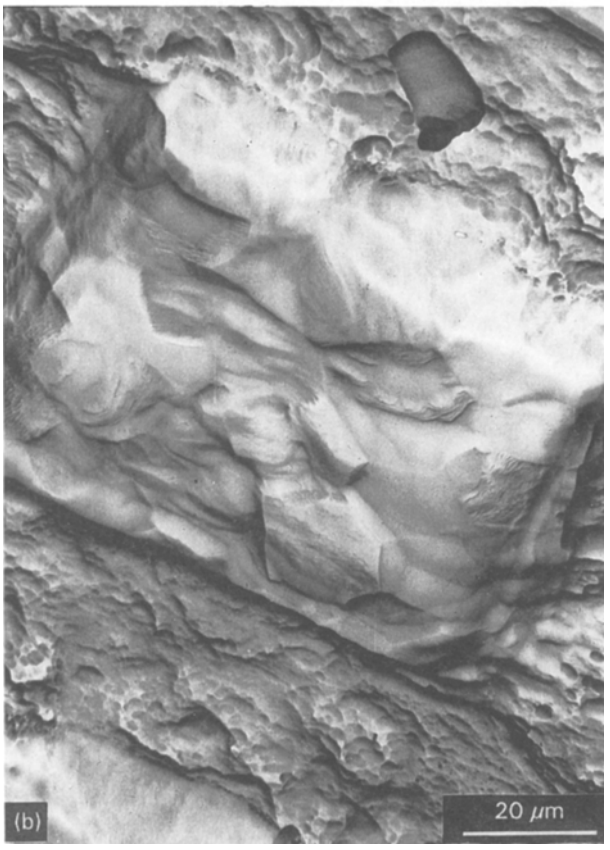

Figure 13 Different aspects of surface topography modification [1] observed by SEM on ion beam pattern etched parts (bottoms of particular depressions) of the polycrystalline 99% titanium sample. (a) Simple elements of a cone texture; (b) revealed surface macrostructure (grains). Ion bombardment conditions as in Fig 12b.

unsputtered and ion bombarded surfaces (measured in the ion beam direction) of the target; and ϕ is ion flux.

From Equations 5–7 it follows that:

$$Y = \frac{nA\,dR}{\phi\,dt} = \frac{n\,dR}{\Phi\,dt} \tag{8}$$

where Φ is the number of ions per second striking the unit area, A.

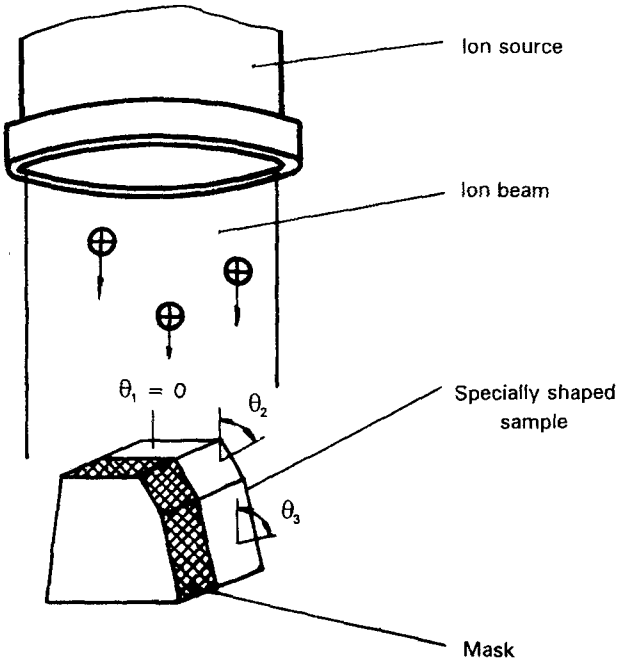

Figure 14 A specially shaped sample with planes partially screened with a sputter-resistant mask, used in the "3S" method of examination of ion beam sputter induced surface shape profile (θ_1, θ_2, θ_3 are angles of ion beam incidence, i.e. the angles between ion beam direction and proper surface normals). $\oplus$ = ion.

According to Equation 8 the breadth

$$dR = \frac{Y\Phi}{n}\,dt \tag{9}$$

but, as can be seen in Fig. 15, it can also be expressed by

$$dR = \frac{dH}{\cos\theta} \tag{10}$$

where dH is the height of step formed on the border between untreated and ion bombarded surface of the target material after unit time of ion beam irradiation.

Combining Equations 9 and 10 gives:

$$dH = \frac{\Phi}{n}\,Y(\theta)\cos\theta\,dt \tag{11}$$

The height H of the step formed after t s of ion beam sputtering, usually measured using a profilograph, can be obtained from Equation 11 after integration over time:

$$H = \int_0^t \frac{\Phi}{n}\,Y(\theta)\cos\theta\,dt = \frac{\Phi t}{n}\,Y(\theta)\cos\theta \tag{12}$$

Using Equation 1, and taking into account

$$N_a = \rho\frac{N_A}{M}V = \rho\frac{N_A}{M}AH \tag{13}$$

and

$$N_i = \frac{It}{e} = \frac{jAt}{e} \tag{14}$$

where ρ is the average target material density in kg m^{-3}; $N_A \approx 6.022 \times 10^{23}$ mol^{-1}; M is the atomic mass of the material in kg mol^{-1}; V is a unit volume of

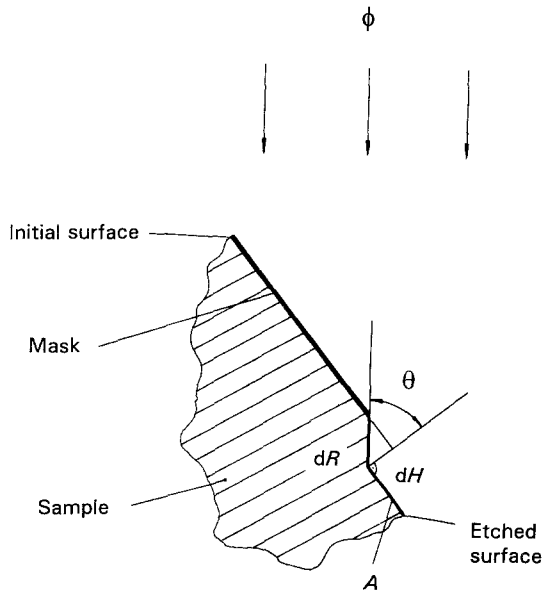

Figure 15 The erosion of unit area, A, of the target surface after unit time, dt, of ion beam bombardment through the sputter-resistant mask. Ion flux is denoted here as ϕ; dR and dH are breadth (measured in ion beam direction) and height of the step formed on the border between etched and untreated surface, respectively; θ is the angle of ion beam incidence [23].

sputtered material in m^{-3}; I is the ion current in A; $e \approx 1.602 \times 10^{-19}$ A s; j is ion current density in $A\,m^{-2}$,
we can write

$$Y = \frac{C}{jt}\frac{\rho}{M}H \tag{15}$$

where

$$C = eN_A \approx 10^5\ A\,s\,mol^{-1} \tag{16}$$

It is clear that for given values of j, t and ρ, M being constant, the sputtering yield Y is a function only of the height H of the step formed on the border between sputtered and untreated surfaces of the perpendicular ($\theta = 0$ rad) plane of a specially shaped sample of the material investigated. The "3S" method enables the sputtering yield Y to be measured for other angles, θ, of ion beam incidence, and the plot $Y(\theta)$ can be obtained.

Using the "3S" method it is also possible to determine the approximate(!) values of sputtering (etching) velocity for various angles θ

$$v(\theta) = \frac{H(\theta)}{t} \tag{17}$$

To obtain the plot $v(\theta)$ it is necessary to define $H(\theta)$. To do this one sputtering process of a specially shaped sample of the material investigated should be made and for each plane (i.e. for each angle $\theta_1, \theta_2, \ldots$, etc.) the height of the step (i.e. $H_1, H_2, \ldots$, etc.) formed during ion bombardment should be measured. In this way a plot for $H(\theta)$ can be obtained, which, after dividing $H(\theta)/t$, gives the plot $v(\theta)$.

Although the method in question is termed as 'approximate' (a lot of phenomena such as scattered and recoil atoms, neutrals in ion beam, redeposited material, etc., are not considered here) the sputtering parameters measured and calculated with the "3S" technique are similar to those obtained elsewhere [23].

5. Conclusion

Two major ion induced surface shape alteration methods, i.e. masked and maskless ion beam pattern etching (IBPE) are described in this paper, both starting at simple, 'classical' techniques and ending at very modern and complicated ones, such as focused ion beam lithography (FIBL) or ion projection lithography (IPL).

Device pattern size has been scaled down every year, therefore demands for high resolution lithography (nanolithography) are continuously increasing. However, Pease [24] states that, "The resolution is not, and never has been, the limiting issue". It seems that throughput, precision and defect density are equally, or even more important, factors. Why do we try to make things smaller and smaller? Pease [24] gives six interesting reasons: (a) it is fun; (b) smaller devices work faster; (c) smaller devices consume less power; (d) smallness is intrinsically good; (e) it is scientifically important; (f) it is cost effective.

Another problem discussed in the paper is approximation of a real surface shape profile by the mean line.

Finally, the application of IBPE induced surface shape profile changes to sputtering yield and velocity measurements are described.

Surface shape alteration together with surface roughness changes (Part 1 [2]) are the main aspects of ion bombardment induced surface geometrical structure modification – these are very complicated and important problems in todays modern technologies, which needs further investigation of the phenomena, mechanisms and questions that should be recognized, solved and discussed.

Acknowledgements

I am much indebted to Mrs. F. Kastraniec for her help in the preparation of this and other papers published in this journal.

References

1. Z. W. KOWALSKI, Science Papers IET TU Wrocław No. 38, Monographs No. 13, edited by PWr (Wrocław, 1989).
2. *Idem, J. Mater. Sci.* **25** (1990) 3875.
3. O. AUCIELLO, in "Ion Bombardment Modification of Surfaces: Fundamentals and Applications", edited by O. Auciello and R. Kelly (Elsevier, Amsterdam, 1984) p. 435.
4. L. F. JOHNSON, ibid., p. 361.
5. I. W. RANGELOW and Z. W. KOWALSKI, *Beitr. elektronenmikroskop. Direktabb. Oberfl.* **15** (1982) 27.
6. A. J. MURAY and J. J. MURAY, *Vacuum* **35** (1985) 467.
7. J. MELNGAILIS, *J. Vac. Sci. Technol.* **B5** (1987) 469.
8. S. NAMBA, *Nucl. Instr. Meth. in Phys. Res.* **B39** (1989) 504.
9. R. A. D. MACKENZIE and G. D. W. SMITH, *Nanotechnology* **1** (1990) 163.
10. M. ŁUKASZEWICZ and Z. W. KOWALSKI, *J. Mater. Sci.* **16** (1981) 302.
11. Z. W. KOWALSKI, J. WILK and W. KRYSIŃSKI, in Proceedings ELTE '90, IV Konferencja Naukowa – Technologia Elektronowa, Książ 11–14.09.1990, Wyd. PWr (Wrocław, 1990) p. 242.

12. W. HAUFFE, in "Sputtering by particle bombardment III", edited by R. Behrisch and K. Wittmack (Springer-Verlag, Berlin, 1991) p. 305.
13. U. S. TANDON, *Vacuum* **43**, 3 (1992) 241.
14. M. PAULUS and F. REVERCHON, *J. Phys. Radium Phys. Appl.* **22**, Suppl. to No. 6 (1961) 103A.
15. R. A. D. MACKENZIE, *J. Vac. Sci. Technol.* **B9**, 5 (1991) 2561.
16. K. GAMO, *Nucl. Instr. Meth. in Phys. Rev.* **B65** (1992) 40.
17. Y. OCHIAI, Y. KOJIMA and S. MATSUI, *J. Vac. Sci. Technol.* **B6**, 4 (1988) 1055.
18. L. R. HARRIOTT, H. TEMKIN, R. A. HAMM, J. WEINER and M. B. PANISH, ibid. **B7**,6 (1989) 1467.
19. K. GAMO, *Vacuum* **42** (1991) 89.
20. P. A. MILLER, *J. Vac. Sci. Technol.* **B7**,5 (1989) 1053.
21. Z. W. KOWALSKI, *J. Mater. Sci. Lett.* **9** (1990) 549.
22. B. A. BANKS, in "Ion bombardment modification of surfaces: fundamentals and applications", edited by O. Auciello and R. Kelly (Elsevier, Amsterdam, 1984) p. 399.
23. Z. W. KOWALSKI, *J. Mater. Sci. Lett.* **6** (1987) 1207.
24. R. F. W. PEASE, *J. Vac. Sci. Technol.* **B10**,1 (1992) 278.

Received 7 October 1992
and accepted 10 December 1993